

Layer-switching cost and optimality in information spreading on multiplex networks

Byungjoon Min^{1,2,*}, Sang-Hwan Gwak^{1,*}, Nanoom Lee¹, and K.-I. Goh^{1,†}

¹Department of Physics, Korea University, Seoul 02841, Korea

²Levich Institute and Physics Department, City College of New York, New York, NY 10031, USA

*these authors contributed equally to this work

†corresponding author: kgoh@korea.ac.kr

ABSTRACT

We study a model of information spreading on multiplex networks, in which agents interact through multiple interaction channels (layers), say online vs. offline communication layers, subject to layer-switching cost for transmissions across different interaction layers. The model is characterized by the layer-wise path-dependent transmissibility over a contact, that is dynamically determined dependently on both incoming and outgoing transmission layers. We formulate an analytical framework to deal with such path-dependent transmissibility and demonstrate the nontrivial interplay between the multiplexity and spreading dynamics, including optimality. It is shown that the epidemic threshold and prevalence respond to the layer-switching cost non-monotonically and that the optimal conditions can change in abrupt non-analytic ways, depending also on the densities of network layers and the type of seed infections. Our results elucidate the essential role of multiplexity that its explicit consideration should be crucial for realistic modeling and prediction of spreading phenomena on multiplex social networks in an era of ever-diversifying social interaction layers.

Introduction

Networks are penetrating ever more deeply through every facet of individual lives and societal functions.¹ At its center, the explosive rise of social media driven by the information communication technology or ICT revolution has profoundly transformed the landscape of human interactions. Human interactions mediated by social media could defy the spatial and temporal limitations of traditional communications in an unprecedented way, thereby offering a qualitatively new layer of social interaction, which coexists and cooperates with existing interaction layers to redefine the multiplex social networks.²⁻⁴ In addition, networks with different types of edges categorized by their relationships have been studied for a long time in social network analysis.⁵⁻⁷ These multiple interaction channels or network layers in a multiplex system do not function completely autonomously nor dependently; while each layer can support some function within its scope, it is the crosstalk and interplay between these layers that can fulfill the full functionality of the system and could give rise to nontrivial and unanticipated collective outcomes such as the recently uprising civil movements in the Middle East.² This poses theoretical challenge as well to extend existing single-network framework⁸⁻¹⁰ by formulating and disseminating the role of multiplex layers that do not always play independent roles in network structure and dynamics, the understanding of which is beginning to be culminated.¹¹⁻¹⁴

Epidemic processes on networks are one of the most actively developed branches in complex network theory,¹⁵ which can address not only the spreading of infectious diseases but also many other contagious phenomena such as information and rumor spreading on social networks. A few recent studies on epidemic spreading beyond the single-network framework have been performed under various terms like overlay networks,¹⁶ multitype networks,¹⁷ interconnected networks,^{18,19} interdependent networks,²⁰ interacting networks,²¹ and multiplex networks.^{22,23} Cascade processes have also been studied on multilayer, interdependent, and multiplex networks.²⁴⁻³⁰ (For details of these terms and their similarity and differences, the reader is referred to the comprehensive table compiled in Ref. 12.) Here we study an epidemic-based information spreading model framework on multiplex social networks, distinguished from existing models by the presence of the layer-switching cost, describing the overburden or surcharge for transmissions that proceed by crossing different layers compared to those proceeding as confined within the same layer. For example, when one received new information through an online social medium, say Twitter, she would more likely spread it again through Twitter as it is most handy, than would do it over other online media, such as e-mail, let alone over an offline social network, as it would require additional effort and/or accompany spatiotemporal delay in switching the medium (network layer). Indeed, early studies using data from Twitter and weblogs have shown that the information diffusion structure is highly platform-dependent.^{31,32} Despite being commonplace, the layer-switching cost has not

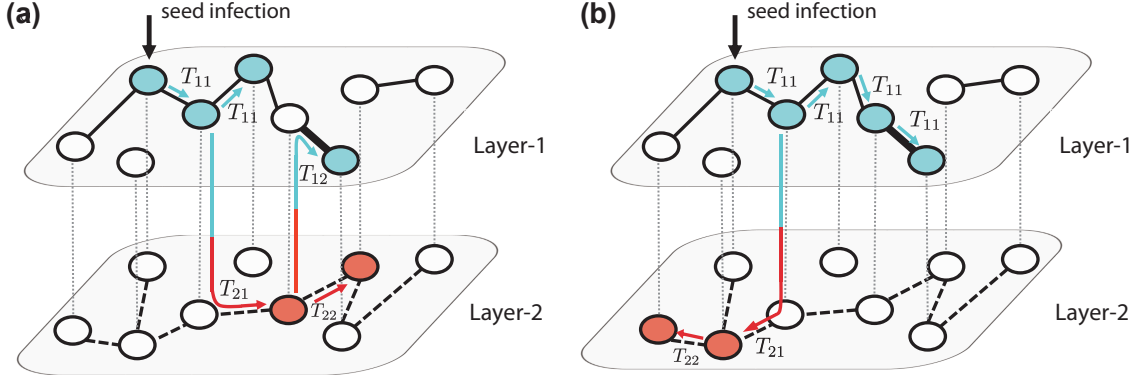


Figure 1. Schematic illustration of the information spreading model with layer-switching cost on the multiplex network with two layers. In this example, the spreading starts with the seed infection in layer 1. Subsequent spreading proceeds with the transmissibility T_{ji} as the transmission in layer j is preceded by the transmission in layer i . Two possible sample spreading trajectories are shown for illustration in (a) and (b), respectively. Nodes are colored according to the type of transmission through which they are infected (blue for type-1 and red for type-2 transmission). Due to the path-dependency, the transmissibility of a given link is not fixed *a priori* but can take different value, as exemplified by the thick link in this figure.

yet been explicitly addressed in multiplex spreading dynamics and thus its implication is not elucidated systematically.

In this paper, we show that this commonplace factor of layer-switching cost can significantly and nontrivially modify information spreading dynamics on multiplex social networks. Most fundamentally, it introduces the path-dependent transmissibility over a contact that is dynamically determined depending on both incoming and outgoing transmission layers, which requires a new theoretical formalism beyond the standard ones.^{33–35} We formulate a generating-function based theory to cope with such path-dependent transmissibility in locally-treelike networks. Using both analytical calculations and numerical simulations, various consequences of the layer-switching cost, and thus the path-dependent transmissibility, are revealed. These include the existence of trade-off between the infection rates along the same layer and across different layers to optimize information spreading for a given average infection rate over different channels and the nearly-confined spreading within the dominant layer when the layer-switching cost is large enough. Our study elucidates how the network multiplexity and the layer-switching cost can alter the information spreading dynamics in non-trivial way and thereby suggests that the modeling neglecting the multiplex social interactions into an aggregated one could potentially mislead to inaccurate conclusions.

The Model

We take account of the effect of network multiplexity and layer-switching cost by introducing the layer-wise path-dependent infection rates. Given more than one layer through which the information or disease spreads, the infection rate for a link (contact) in one layer depends not only on the current layer but also on which layer the information or disease has transmitted from (as in the case of the Twitter example in the previous section). To implement this idea specifically, we construct a model based on the prototypical susceptible-infected-recovered (SIR) model framework for epidemic spreading³⁶ taking place on multiplex networks with more than one layer. In the SIR model, each node is in one of three states, susceptible, infected, or recovered (or removed). An infected node can spread information (or rumor or disease) to a susceptible neighbor with the infection rate β , and each infected node is recovered after a time τ from the moment of infection. We here assume that the probability distribution of the recovery time τ is sharply peaked, and so well-described by the delta function. The probability that an infected agent infects its neighbors before recovery, denoted by T , is called the transmissibility, which is, under the above assumption, given by $T = 1 - e^{-\beta\tau} = 1 - e^{-\lambda}$,³³ defining the dimensionless parameter $\lambda \equiv \beta\tau$ as the effective infection rate. The average fraction of recovered nodes in the stationary state ($t \rightarrow \infty$ limit), ρ , is called the prevalence and is the main observable in the spreading process.

For the spreading process on a multiplex network with in general ℓ layers, we define the type- i transmission to be the infection event in which the infection occurs through a link in layer i ($i = 1, 2, \dots, \ell$). The key feature of our model is that the infection rate over a link depends on the types of both incoming (preceding) and outgoing (current) infection layers. To be specific, when a node is infected via a type- i transmission, then the effective infection rate for the infection through the same layer link (type- i transmission) is λ_{ii} whereas that through a link in different layer j (type- j transmission) is λ_{ji} , where these infection rates are different in general. With the interest on the effect of layer-switching cost, we mainly consider the case

$\lambda_{ii} \geq \lambda_{ji}$, yet the model framework itself does not impose any such constraint. As a consequence of layer-wise path-dependent infection rates in our model, the transmissibilities T_{ij} become accordingly dependent on the types of both incoming and outgoing infection layers. Therefore, the transmissibility through a given link is not fixed *a priori* but can change as the spreading dynamics proceeds, as exemplified in Fig. 1.

Analytical framework

In this section we develop an analytical framework for our model applicable to the case of the multiplex network of locally-treelike random network layers, based jointly on the well-established single-network framework for SIR models^{33–35} as well as the percolation on multiplex networks.^{37–41} (While our theory is strictly derived from the assumption of locally-treelike random networks, the theoretical approach may also apply to some non-treelike real networks as reported in Ref. 42.) For the sake of explicit illustration, our discussion proceeds for the simplest case of 2-layer (duplex) networks, and the generalization to $\ell > 2$ layers is straightforward.

Outbreak size

We first consider the average epidemic size once the epidemic outbreak occurs, denoted S and called the outbreak size, equivalent to the average nonzero final fraction of recovered nodes. According to the standard theory,^{34,35} in order to estimate the outbreak size S one needs the incoming transmissibility of each type of links, which however is not given *a priori* in our model. In our model, the incoming transmissibility for a link is not assigned inherently and definitively but determined dynamically and dependently on the transmission channel by which the infecting node had become infected. In what follows we tackle this difficulty by using a method based on the self-consistency argument to infer the effective incoming transmissibility yielding the same outbreak size S as the original problem.

In order to infer the effective incoming transmissibility for each kind of links, we first estimate the probability π_{ij} that an infected node reached by following a randomly-chosen type- i link had been infected by a type- j transmission. This probability π_{ij} can be expressed in terms of the probability $\pi_{ij}^{(k_1, k_2)}$ that an infected node with the multiplex degree (k_1, k_2) reached by following a randomly-chosen type- i link had been infected by a type- j transmission as $\pi_{ij} = \sum_{k_1=0, k_2=0}^{\infty} \frac{k_i p(k_1, k_2)}{z_i} \pi_{ij}^{(k_1, k_2)}$, where z_i is the mean degree of the layer i . In our model, there are two different possible ways that a node is infected by a type- i transmission: the node could be infected by a neighbor which had been infected either by a type- i or type- j transmission, with respective transmissibilities, T_{ii} and T_{ij} . For locally-treelike layers this consideration leads that $\pi_{ij}^{(k_1, k_2)}$ and $\pi_{ii}^{(k_1, k_2)}$ are respectively proportional to $k_j(T_{ji}\pi_{ji} + T_{jj}\pi_{jj})$ and $(k_i - 1)(T_{ii}\pi_{ii} + T_{ij}\pi_{ij})$. Summing up for the multiplex degree and properly normalizing lead to the coupled self-consistency equations for π_{ij} 's, given by

$$\begin{aligned} \pi_{ii} &= \frac{\kappa_i}{\pi_i} (T_{ii}\pi_{ii} + T_{ij}\pi_{ij}), \\ \pi_{ij} &= \frac{\mathcal{K}_i}{\pi_i} (T_{ji}\pi_{ji} + T_{jj}\pi_{jj}), \end{aligned} \quad (1)$$

where

$$\kappa_i = (\langle k_i^2 \rangle - z_i)/z_i, \quad \mathcal{K}_i = \langle k_i k_j \rangle / z_i,$$

and π_i is the normalization factor imposed by $\pi_{ii} + \pi_{ij} = 1$, for distinct $i, j \in \{1, 2\}$. Solving these equations for π_{ij} 's with given $p(k_1, k_2)$ and T_{ij} 's (equivalently, λ_{ij} 's), one can obtain the effective average incoming transmissibility through the type- i link, denoted \tilde{T}_i and given by

$$\tilde{T}_i = T_{ii}\pi_{ii} + T_{ij}\pi_{ij}. \quad (2)$$

What is achieved thus far is to transform the original model into an equivalent (with respect to S) SIR model with (path-independent) transmissibility \tilde{T}_i in each layer i . The outbreak size of the transformed model can be found in the standard way, by adapting the methods developed for percolation in multiplex networks.^{37–40} Let $G_0(x, y)$ be the generating function of the joint degree distribution $p(k_1, k_2)$, $G_0(x, y) = \sum_{k_1=0, k_2=0}^{\infty} p(k_1, k_2) x^{k_1} y^{k_2}$. The generating function $G_0(x, y; p, q)$ of the joint distribution of the numbers of occupied edges when the edges are independently occupied with the probability p in layer 1 and q in layer 2 can be written as $G_0(x, y; p, q) = G_0(1 + (x-1)p, 1 + (y-1)q)$. In the transformed SIR model the edges in layer i are occupied with probability \tilde{T}_i , so the probability that a node reached by following a randomly-chosen type- i link does not belong to the epidemic outbreak, denoted x_i , is given by³³

$$x_i = \frac{1}{z_i \tilde{T}_i} \frac{\partial}{\partial x_i} G_0(x_1, x_2; \tilde{T}_1, \tilde{T}_2) \quad (3)$$

with $i = 1, 2$. Finally, the outbreak size S (that is, the probability that a random-chosen infected node belongs to the giant connected component of infected nodes) can be obtained as

$$S = 1 - G_0(x_1, x_2; \tilde{T}_1, \tilde{T}_2), \quad (4)$$

with x_i 's being the physical solution of Eq. (3).

Outbreak probability

The outbreak probability can be in general different with the outbreak size due to the effective directionality induced by the path-dependent transmissibility in our model.^{34,35} In order to obtain the outbreak probability, we can follow the path-dependent transmissibilities determined by the incoming and the outgoing transmission channels explicitly. Let y_i be the probability that a node infected by type- i transmission does not lead to an epidemic outbreak. Similarly to Eq. (3), y_i 's satisfy the coupled self-consistency equations

$$y_i = \frac{1}{z_i T_{ii}} \frac{\partial}{\partial y_i} G_0(y_1, y_2; T_{1i}, T_{2i}), \quad (5)$$

with $i = 1, 2$. The probability P_i that a type- i seed infection gives rise to an epidemic outbreak (that is, the infection spreads indefinitely) is then given by

$$P_i = 1 - G_0(y_1, y_2; T_{1i}, T_{2i}), \quad (6)$$

with y_i 's being the physical solution of Eq. (5). Note that unlike the outbreak size S , the outbreak probability P_i depends on which layer the epidemic is initiated from.

Epidemic threshold

The epidemic threshold can be obtained by the linear stability criterion of the trivial fixed point $(y_1, y_2) = (1, 1)$ of Eq. (5). The condition of the epidemic outbreak requires the largest eigenvalue Λ of the Jacobian matrix \mathbf{J} of Eq. (5) at $(1, 1)$ to be larger than unity, $\Lambda > 1$, which is the condition of the fixed point being unstable. The Jacobian matrix \mathbf{J} at $(1, 1)$ can be simply expressed as

$$\begin{pmatrix} T_{11} \kappa_1 & T_{21} \kappa_1 \\ T_{12} \kappa_2 & T_{22} \kappa_2 \end{pmatrix}. \quad (7)$$

The largest eigenvalue Λ can be explicitly calculated as

$$\Lambda = \frac{1}{2} \left[T_{11} \kappa_1 + T_{22} \kappa_2 + \sqrt{(T_{11} \kappa_1 - T_{22} \kappa_2)^2 + 4T_{12} T_{21} \kappa_1 \kappa_2} \right]. \quad (8)$$

Note that $\Lambda \geq \max(T_{11} \kappa_1, T_{22} \kappa_2)$, meaning that the epidemic threshold of the multiplex network cannot be larger than the epidemic thresholds of individual layers.

Comparison with numerical simulations

To verify the validity of the proposed analytical framework, we compare the analytical calculation with the numerical simulation results. The numerical simulation of our model proceeds as follows. Initially, all nodes are susceptible except for one randomly-chosen seed which is assumed to be infected by a type- i transmission (that is, infected through layer i). Infected nodes transmit the disease to their susceptible neighbors with the infection rates λ_{ji} determined by both the incoming channel i and the outgoing channel j . Each infected node recovers after a fixed recovery period, τ . The spreading process proceeds until all infected nodes in the network recover, which completes one independent run of the numerical simulation. After many independent runs, we compute the outbreak probability P_i as the fraction of runs ending up with the fraction of recovered nodes above the prescribed threshold (chosen to be 1% in our numerical simulation). Likewise the outbreak size S is computed as the average of the fraction of recovered nodes above the threshold. The prevalence due to type- i seed infection, ρ_i , is computed as $\rho_i = P_i S$.

Duplex ER networks

To gain further insights on the role of layer-switching cost, we elaborate further on analyzing the model on the 2-layer network formed by two independently-constructed Erdős-Rényi (ER) layers (henceforth the duplex ER network, for short), for which one can obtain the analytical results in an explicit form. Mean degrees of two ER layers are denoted z_1 and z_2 , respectively. To

focus on the effect of layer-switching cost, we further simplify the parameter setting such that the infection rates within the same layer are equal as $\lambda_{11} = \lambda_{22} \equiv \lambda_s$ (“s” for same) and similarly for the infection rates across different layers as $\lambda_{12} = \lambda_{21} \equiv \lambda_d$ (“d” for different). Corresponding transmissibilities are given by $T_i = 1 - e^{-\lambda_i}$, where i is either s or d . We further assume $\lambda_s \geq \lambda_d$, so that the information spreading along the same layer is easier than that across layers, in compliance with the concept of layer-switching cost.

When the two layers are randomly-coupled, the effective incoming transmissibilities can be calculated under this simplified setting as

$$\tilde{T}_1 = \frac{T_s}{2} - \frac{z_2 T_d}{z_1 - z_2} + \sqrt{\frac{T_s^2}{4} + \frac{z_1 z_2 T_d^2}{(z_1 - z_2)^2}} \quad \text{and} \quad \tilde{T}_2 = \frac{T_s}{2} + \frac{z_2 T_d}{z_1 - z_2} - \sqrt{\frac{T_s^2}{4} + \frac{z_1 z_2 T_d^2}{(z_1 - z_2)^2}}. \quad (9)$$

Using $G_0(x, y) = e^{z_1(x-1) + z_2(y-1)}$ for randomly-coupled duplex ER networks, Eqs. (3) and (4) are reduced to a single equation for $x_1 = x_2 = 1 - S$, so that the outbreak size S is given by the solution of

$$1 - S = e^{-(z_1 \tilde{T}_1 + z_2 \tilde{T}_2)S}. \quad (10)$$

Similarly for the epidemic probability, Eqs. (5) and (6) are reduced to two coupled equations for $y_i = 1 - P_i$, given by

$$\begin{aligned} 1 - P_1 &= e^{-(z_1 T_s P_1 + z_2 T_d P_2)}, \\ 1 - P_2 &= e^{-(z_1 T_d P_1 + z_2 T_s P_2)}. \end{aligned} \quad (11)$$

As shown in Fig. 2a, for randomly-coupled duplex ER networks the proposed analytical calculation results exhibit good agreement with the numerical simulation results even for the networks with moderate size $N = 10^4$, supporting the validity of the analytic framework. Deviations observed near the epidemic threshold are due to the finite size. Moreover the results in Fig. 2a manifest clearly that the outbreak probability P_i and size S can be different each other above the epidemic threshold. It can also be noted that P_1 and P_2 can be different each other so that the outbreak probability and prevalence above the epidemic threshold does depend on the layer from which the infection is initiated.

Assessing the effect of layer-switching cost

To assess the effect of layer-switching cost in minimal way, we employ a new parametrization for the infection rates and the mean degrees as follows. First, the infection rates are parameterized by

$$\lambda_s = (1 + \delta\lambda)\lambda \quad \text{and} \quad \lambda_d = (1 - \delta\lambda)\lambda. \quad (12)$$

Here λ is the average infection rate and $0 \leq \delta\lambda \leq 1$ accounts for the level of layer-switching cost, such that $\lambda_s \geq \lambda_d$. By this parametrization we consider the scenario in which one could modulate the difference in λ_s and λ_d with $\delta\lambda$ while the average infection rate is kept fixed by the total amount of resource for information spreading. Similarly, the mean degrees of the two layers are parametrized as $z_1 = (1 + \delta z)z_0/2$ and $z_2 = (1 - \delta z)z_0/2$. Here z_0 is the total mean degree of the two layers and $0 \leq \delta z \leq 1$ quantifies the disparity in the link density of the two layers. By using this parametrization we aim to assess the effect of layer-switching cost as the relative link density of two layers changes while the total number of links is kept fixed.

To have the first sense for the effect of layer-switching cost, we take a look at the information spreading dynamics on duplex ER networks initiated from a type-1 transmission for several values of $\delta\lambda$. Two values of link density disparity $\delta z = 0$ and $\delta z = 1/2$ for the same total degree $z_0 = 2.5$ (equivalently, $z_1 = 1.875$ and $z_2 = 0.625$) are chosen for comparison. As shown in Fig. 2, the effect of layer-switching cost is multifaceted, depending on the network (parametrized by δz here) as well as which aspect of information spreading one is interested in. For $\delta z = 0$, the effect is rather simple: the layer-switching cost tends to hinder the information spreading, in that the larger $\delta\lambda$ is, the larger is the epidemic threshold λ_c as well as the smaller is the prevalence ρ (Fig. 2b). For $\delta z = 1/2$, however, the effect of layer-switching cost is more intricate (Fig. 2c). As $\delta\lambda$ increases from zero, the epidemic threshold becomes smaller, meaning that the epidemic outbreak is facilitated near the threshold. On the contrary, larger $\delta\lambda$ yields smaller value of prevalence ρ when λ is sufficiently larger than the epidemic threshold. For large enough λ the system is well percolated, so large value of layer-switching cost causing confinement of epidemic spreading within the initial layer hinders the effective use of entire available network and thus produces suppressive effect. What happens for small λ is instead that the confined spreading within the denser layer due to large layer-switching cost becomes advantageous by avoiding the trapping of spreading in the sparse layer below percolation threshold. In this way, the layer-switching cost can lead to apparently counteracting effect depending on the average infection rate λ . Numerical simulation and theoretical calculation for different total mean degree $z_0 = 1.25$ and $z_0 = 5.0$ with $\delta z = 1/2$, for which both the layers are unpercolating (percolating) for the former (latter), show qualitatively similar pattern (Figs. 2d,e).

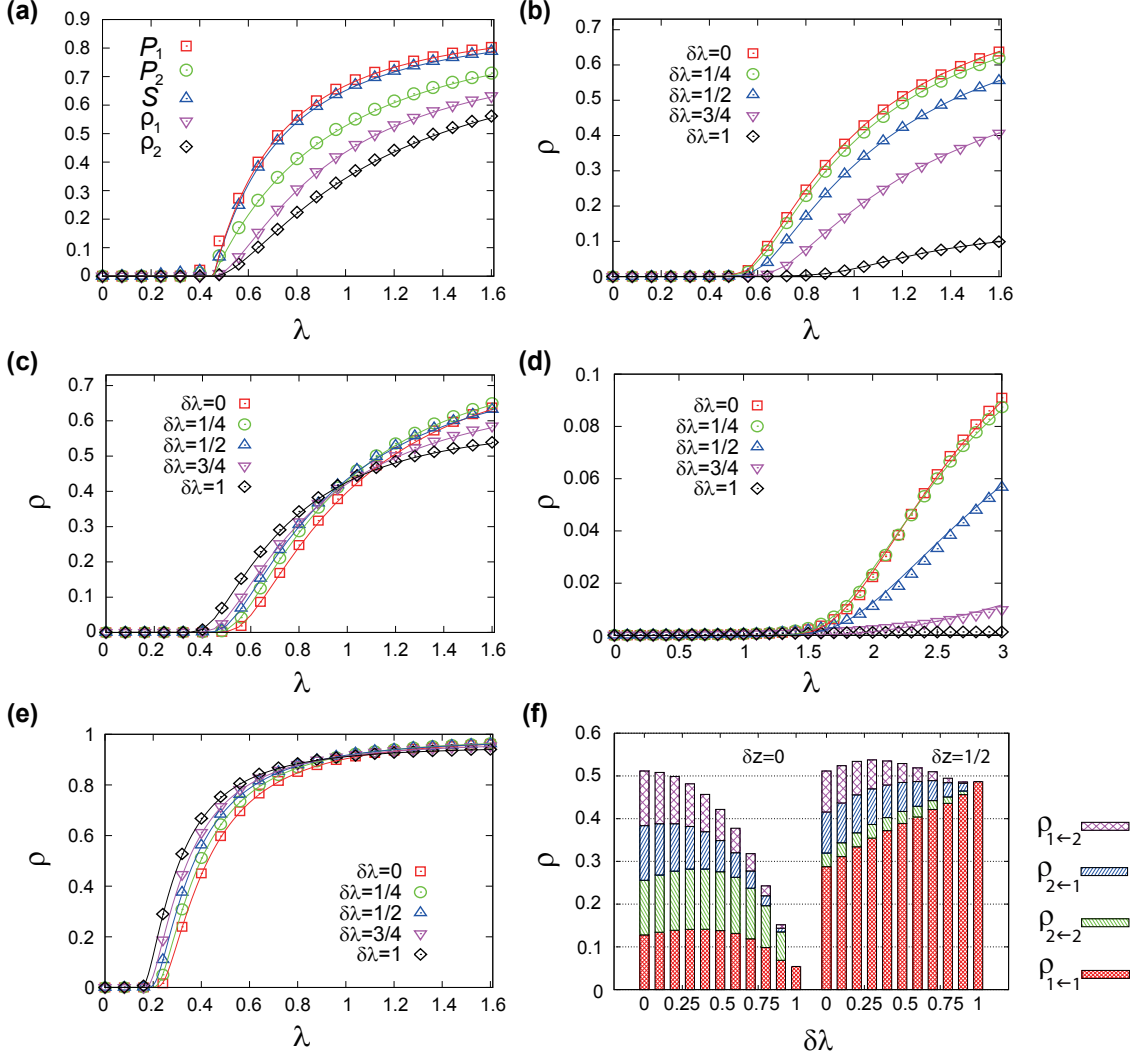


Figure 2. (a) Comparison of the analytical calculation (lines) and numerical simulation (symbols) results for the outbreak probabilities P_1 (\square) and P_2 (\circ), the outbreak size S (\triangle), and the prevalence ρ_1 (∇) and ρ_2 (\diamond), plotted as a function of λ . The results are for the duplex ER networks with $z_0 = 2.5$, $\delta z = 1/2$, and $\delta\lambda = 1/2$. Numerical simulation results are obtained with $N = 10^4$ nodes. (b, c) The prevalence ρ on duplex ER networks with $z_0 = 2.5$, $\delta z = 0$ (b) and $\delta z = 1/2$ (c) for several values of cost parameter $\delta\lambda = 0$ (\square), $1/4$ (\circ), $1/2$ (\triangle), $3/4$ (∇), and 1 (\diamond). Theoretical curves (lines) and numerical results obtained with $N = 10^4$ nodes (points) are shown together. (d, e) The plots of prevalence ρ on duplex ER networks with $\delta z = 1/2$ for $z_0 = 1.25$ (d) and $z_0 = 5.0$ (e) for several values of cost parameter $\delta\lambda$. Same symbols and lines as panels b and c are used. (f) The infection path profile in terms of the stacked histogram of the epidemic outbreak size different infection channels ρ_{ji} for duplex ER networks of $z_0 = 2.5$ and $\delta z = 0$ (left) and $\delta z = 1/2$ (right), with $\lambda = 1.2$ and various values of $\delta\lambda$.

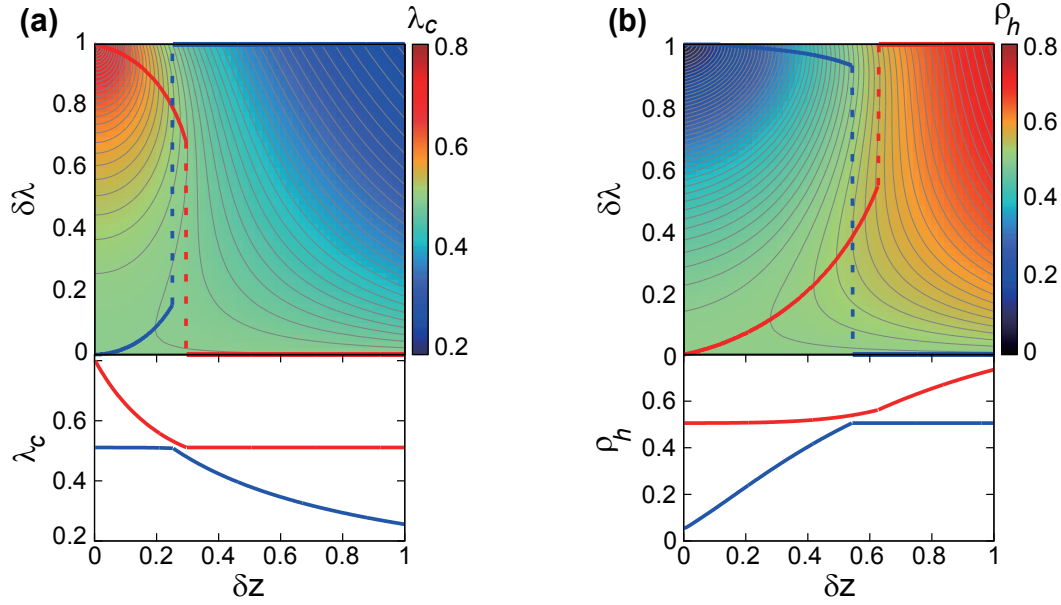


Figure 3. The epidemic threshold λ_c (a) and the prevalence for $\lambda = 1.2$ denoted as ρ_h (b) as a function of δz and $\delta \lambda$ for the randomly-coupled duplex ER network with $z_0 = 2.5$ are density-plotted in the top panels. Thick red (blue) line in top panels is the trace of the loci of maximum (minimum) value of λ_c (a) and ρ_h (b) with respect to $\delta \lambda$ at the given δz , which can undergo discontinuous jump upon changing δz , indicated by the dashed line. At the bottom panels, the values of the maximal (red) and minimal (blue) λ_c (a) and ρ_h (b) with respect to $\delta \lambda$ are plotted as a function of the given δz .

Infection channel profile

The unequal usage of different transmission channels arises from the link density and the layer-switching cost. To quantify this we make the infection channel profile consisting of epidemic outbreak sizes due to each channel $\rho_{i \leftarrow j}$, which can be computed by the fraction of each transmission channels T_{ij} is used during the information spreading process. In Fig. 2f we show the infection channel profiles for the previously-examined two cases of duplex ER networks of $z_0 = 2.5$ with $\delta z = 0$ and $\delta z = 1/2$ (corresponding to Figs. 2b and c), respectively. We take $\lambda = 1.2$, well above the threshold. For $\delta z = 0$, as the layer-switching cost parameter $\delta \lambda$ increases the use of cross-layer transmission channels is suppressed more significantly whereas the intra-layer channels remain used in a similar level as long as $\delta \lambda < 1$, illustrating clearly the simple detrimental role of layer-switching cost for $\delta z = 0$. For $\delta z = 1/2$, on the other hand, the total epidemic size ρ is more or less insensitive to $\delta \lambda$ while the composition of $\rho_{i \leftarrow j}$ significantly and systematically varies, with the intra-layer channel through denser layer $\rho_{1 \leftarrow 1}$ increasingly dominating the spreading as $\delta \lambda$ increases.

Epidemic threshold and prevalence

To establish a more comprehensive picture, we compute the epidemic threshold and the prevalence for the full range of $\delta \lambda$ and δz . We specifically consider the prevalence ρ_h computed for $\lambda = 1.2$, well above the threshold, to address the situation where the level of available infection capacity is high enough for large-scale spreading. Therefore the two quantities could be a relevant measure for the efficacy of information spreading when the available infection capacity is tightly limited and sufficiently rich, respectively.

Plots of the epidemic threshold λ_c and the prevalence ρ_h for the duplex ER networks with $z_0 = 2.5$ are shown in Fig. 3. In Fig. 3a, we also indicate in the upper panel the loci of $\delta \lambda$ producing the largest threshold (λ_c^{\max} , red) and smallest threshold (λ_c^{\min} , blue) for given δz . The corresponding maximal and minimal λ_c as a function of δz is shown in the lower panel. The loci of $\delta \lambda$ for maximal and minimal λ_c jumps abruptly at $\delta z = 0.297$ and $\delta z = 0.253$, respectively, which is accompanied by the discontinuity of the first derivative in the plots of λ_c^{\max} and λ_c^{\min} vs. δz .

Similarly, in Fig. 3b, we display in the upper panel the loci of $\delta \lambda$ producing the largest (red) and smallest (blue) ρ_h for given δz . The corresponding largest and smallest prevalence ρ_h as a function of δz is shown in the lower panel. The loci of $\delta \lambda$ for maximal and minimal ρ_h also undergo abrupt jump at $\delta z = 0.672$ and $\delta z = 0.543$, respectively, which is associated with the discontinuity of the first derivative in the plots of ρ_h^{\max} and ρ_h^{\min} vs. δz .

Taken together, the effect of layer-switching cost demonstrated by Fig. 3 can be summarized as follows. First, its effect is

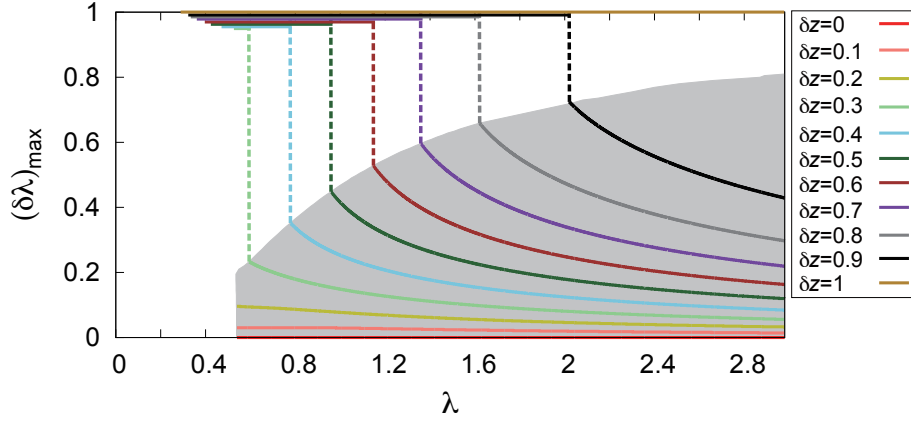


Figure 4. Plot of optimal cost parameter $(\delta\lambda)_{\max}$ for maximizing prevalence ρ as a function of λ with several values of δz . The optimal parameter for information spreading with a limited resource (given λ) exhibits an abrupt discontinuous change for a wide range of δz . Note that all the $(\delta\lambda)_{\max}$'s below the discontinuous transition point are exactly 1 and overlapping; here we have purposefully split them next to each other for visual convenience.

rather simple either when the two layers have similar density ($\delta z \lesssim 0.2$) or when the network density disparity is high enough ($\delta z \gtrsim 0.7$). In such cases, its effect is largely monotonic: either suppressive or facilitative for information spreading, albeit the effect is reversed for small and large disparity. On the other hand, for intermediate range of disparity ($0.2 \lesssim \delta z \lesssim 0.7$), the effect of layer-switching cost is no longer simple. Its effect is non-monotonous as well as it can accompany an abrupt, substantial discontinuity in the optimal parameter under a slight change of network density disparity. In sum, since the layer-switching cost tends not just to hinder cross-layer transmissions but also to promote intra-layer transmissions, the relative contribution and tradeoff between the two effects subject to the given network parameters and the level of available infection capacity can result in non-trivial and non-monotonic consequences to information spreading dynamics on multiplex networks, leading us to the concept of optimality.⁴³

Optimal layer-switching cost for maximal spreading

The intricate effect of layer-switching cost allows formulation of many different optimization problems, contingent upon the objective of optimization as well as the given network parameters. In this section we analyze one particular optimization problem of finding the optimal layer-switching cost $(\delta\lambda)_{\max}$ that maximizes the prevalence for given total infection capacity dictated by λ , as an illustrative example.

In Fig. 4, we show the optimal cost $(\delta\lambda)_{\max}$ as a function of λ computed for duplex ER networks of $z_0 = 2.5$. When $\delta z < 0.280$, small value of $\delta\lambda$, that is, layer-indiscriminate spreading, is advantageous for any λ above the threshold. On the other hand, when $\delta z > 0.280$, the optimal parameter $(\delta\lambda)_{\max}$ changes sensitively to λ . Moreover, it undergoes an abrupt discontinuous change at some λ , whose location depends on δz , below which it is always advantageous to concentrate the spreading through the denser layer, that is, $(\delta\lambda)_{\max} = 1$, down to the threshold λ_c for spreading. The locations of the abrupt change in $(\delta\lambda)_{\max}$ constitute the boundary of shaded region in Fig. 4. This example demonstrates explicitly how the non-analytical and discontinuous response of spreading dynamics to the layer-switching cost in multiplex networks can manifest generically in optimizing information spreading on multiplex networks. Optimization problems with other objectives such as minimizing the epidemic threshold for given network disparity can also be analyzed readily in this framework.

Effect of interlayer degree correlations

In investigating the effect of layer-switching cost so far we have only considered the spreading processes on randomly-coupled multiplex networks, in which the degrees of a node in different layers are uncorrelated. For many real-world networks, however, layers of a multiplex network often do not combine randomly. One of the simplest manifestation of the correlated coupling of multiplex layers is the interlayer degree correlation, that the degrees of a node at different layers are correlated, the effect of which has been examined for the robustness and controllability of multiplex networks.^{27,40,44}

We illustrate the effect of interlayer degree correlation by using duplex ER networks with three representative cases of interlayer correlated coupling:^{38,40} Given two layers, we couple the layers in the maximally-correlated way by coupling the two nodes from each layer in their degree order; in the maximally-anticorrelated way by coupling the nodes in the opposite degree order; or just randomly in uncorrelated way (Fig. 5a). Consequently, a node that is the hub in one layer is also the hub in the other layer for the maximally-correlated case, but it has the smallest degree in the other layer for the maximally-negative case.

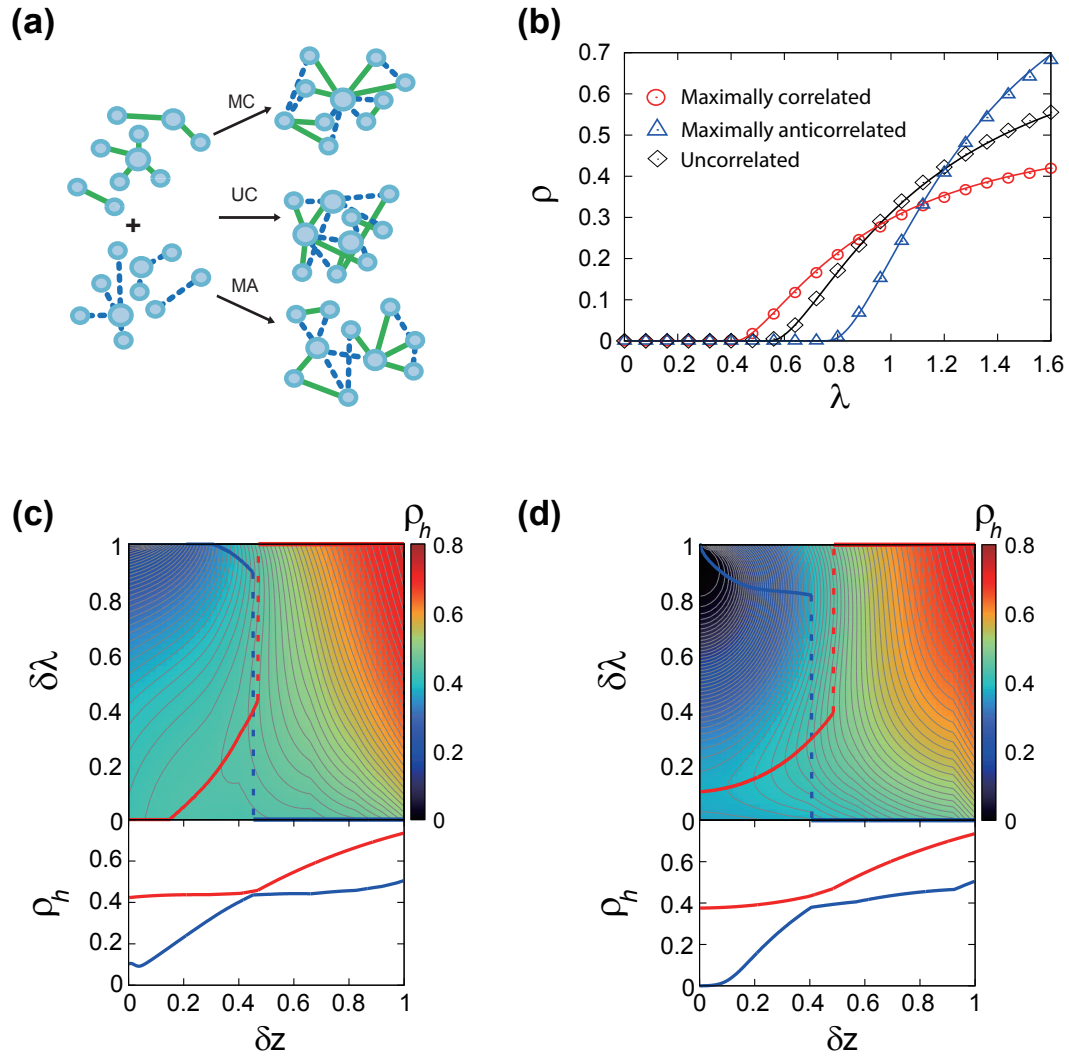


Figure 5. (a) Schematic cartoon illustrating the interlayer degree correlated couplings considered in the text. MC stands for maximally correlated, UC for uncorrelated, and MA for maximally anti correlated. (b) Plots of epidemic prevalence ρ on maximally-correlated (\circ), maximally-anticorrelated (\triangle), and uncorrelated (\diamond) duplex ER networks with $z_0 = 2.5$ and $\delta\lambda = 1/2$, as a function of λ . Numerical results obtained with $N = 10^4$ nodes (points) and theoretical curves (lines) are in good agreement. (c, d) The prevalence ρ_h for $\lambda = 1.2$ on the maximally-correlated (c) and maximally-anticorrelated (d) duplex ER networks with $z_0 = 2.5$, together with the maximum (red) and minimum (blue) ρ_h plotted in the lower panels as a function of δz .

We show the prevalence plot for duplex ER networks of layers with equal mean degree $5/4$ ($z_0 = 5/2, \delta z = 0$) and with layer-switching cost $\delta\lambda = 1/2$ in Fig. 5b and for the entire range of $\delta\lambda$ and δz in Figs. 5c,d, as illustrative example. In this case, the largest eigenvalue of the Jacobian matrix has the simple expression as $\Lambda = T_s \kappa + T_d \mathcal{K}$, where κ and \mathcal{K} are the self- and cross-second moments, respectively, of the joint degree distribution defined in Eq. (1). This indicates that the epidemic threshold should decrease with the interlayer degree correlation, codified by \mathcal{K} , confirmed in Fig. 5b that λ_c is lowest for the maximally-correlated case and highest for the maximally-anticorrelated case. For the large enough λ , by contrast, the prevalence ρ becomes largest for maximally-anticorrelated case and smallest for maximally-correlated case. Therefore, the interlayer degree correlation facilitates the emergence of epidemics (lowering λ_c) but at the same time hinders the large-scale epidemic for high transmissibilities (smaller ρ), reminiscent of the effect of degree assortativity in single-layer networks.⁴⁵ For the intermediate case, the response of the epidemic prevalence with respect to interlayer degree correlation is more complicated and dependent on details, as exemplified in Figs. 5c,d for the maximally-correlated (c) and maximally-anticorrelated (d) cases, respectively.

Empirical Twitter network

We simulate the model on the empirical multiplex network constructed from Twitter data in Ref. 4. This network consists of two layers, the retweet layer and the reply layer (Fig. 6a). Each node is a Twitter account and two nodes are connected in the retweet layer if one “retweets” the other’s tweet message at least once and in the reply layer if one “replies” to the other’s tweet at least once. Although these two layers do not represent different communication media or platforms but different modes of usage of the common medium, Twitter, considering them from a functional point of view they are relatively autonomous, in that the flow of information is likely confined within the given mode and only occasionally crosses to the different mode: One is more likely to retweet the information seen from other’s retweet message than to reply it to someone else. It can therefore be addressed, at least schematically, by the model with layer-switching cost. Moreover, this dataset is one of the rare multiplex social network dataset which is publicly-available yet sufficiently large-scale, thus suitable for the modeling study. The network contains $N = 456,631$ nodes and the mean degrees of the two layers are $z_{\text{retweet}} = 3.21$ and $z_{\text{reply}} = 1.92$, corresponding to $z_0 = 5.13$ and $\delta z = 0.25$. The degree distribution of each layer is fitted to a power law with the exponent ≈ -2.3 (Fig. 6b).

We show the simulation results of the prevalence ρ as a function of λ (Fig. 6c) and the infection channel profile with $\lambda = 1.2$ (Fig. 6d) for different $\delta\lambda$. On this network, the layer-switching cost is found advantageous for information spreading in wide range of $\lambda > 0$, until λ becomes large enough ($\lambda \gtrsim 2.5$) when no appreciable differences are observed for different $\delta\lambda$. Infections through the retweet layer predominate the epidemic process, as this layer is denser. Compared with the model network results on duplex ER networks (Fig. 2), two notable structural features of the Twitter network are worth to be highlighted. First, the broad degree distribution of the Twitter network brings the epidemic threshold close to zero,⁴⁶ so that the effect of layer-switching cost on changing the epidemic threshold is not observable. Secondly, structural organization of the two layers are not completely independent; rather they are highly correlated, since people tend to reply to someone who she/he had retweeted. In effect, there is prevalence of link overlap⁴⁷ across the two layers. In the current dataset, 73.2% of reply links are overlapping with retweet links and the size of giant connected component of the two-layer network is dominated by the retweet layer. This feature severely constrains the effect of outbreak suppression for large λ . Overall, the effect of layer-switching cost on the empirical Twitter data network is moderate yet non-negligible. Notably, when λ is not too large ($\lambda \lesssim 1$), it can induce change in the prevalence by as large as 10 to 50% (Fig. 6c, inset). The interplay of other higher-order structural features present in real-world networks, such as clustering and community structure⁴⁸ and evolution-driven correlation,^{49,50} for information spreading dynamics remains to be investigated further.

Infection Rates Dependent on Source Layer

Although motivated originally to address the effect of layer-switching cost, the present model framework is applicable more broadly to the generic class of spreading processes involving layer-wise path-dependent transmissibilities. One such case is where the infection rates are still path-dependent but determined primarily by the source layer. For example, one may have the infection rates parametrized as

$$\lambda_{j1} = (1+c)\lambda_0 \quad \text{and} \quad \lambda_{j2} = (1-c)\lambda_0 \quad (13)$$

with $-1 \leq c \leq 1$. In the context of information spreading, such parameter setting may arise when a particular social layer (the layer 1 for $c > 0$) has much higher credibility than the other so that the information received in that layer is taken more seriously and so more likely to be passed on through either layer whereas the information received in the other layer gets less attention and likely disregarded.

We perform analysis of the model with infection rates given by Eq. (13) on randomly-coupled duplex ER networks. The prevalence tends to be larger in this model than that for the original model with layer-switching cost, Eq. (12), while the

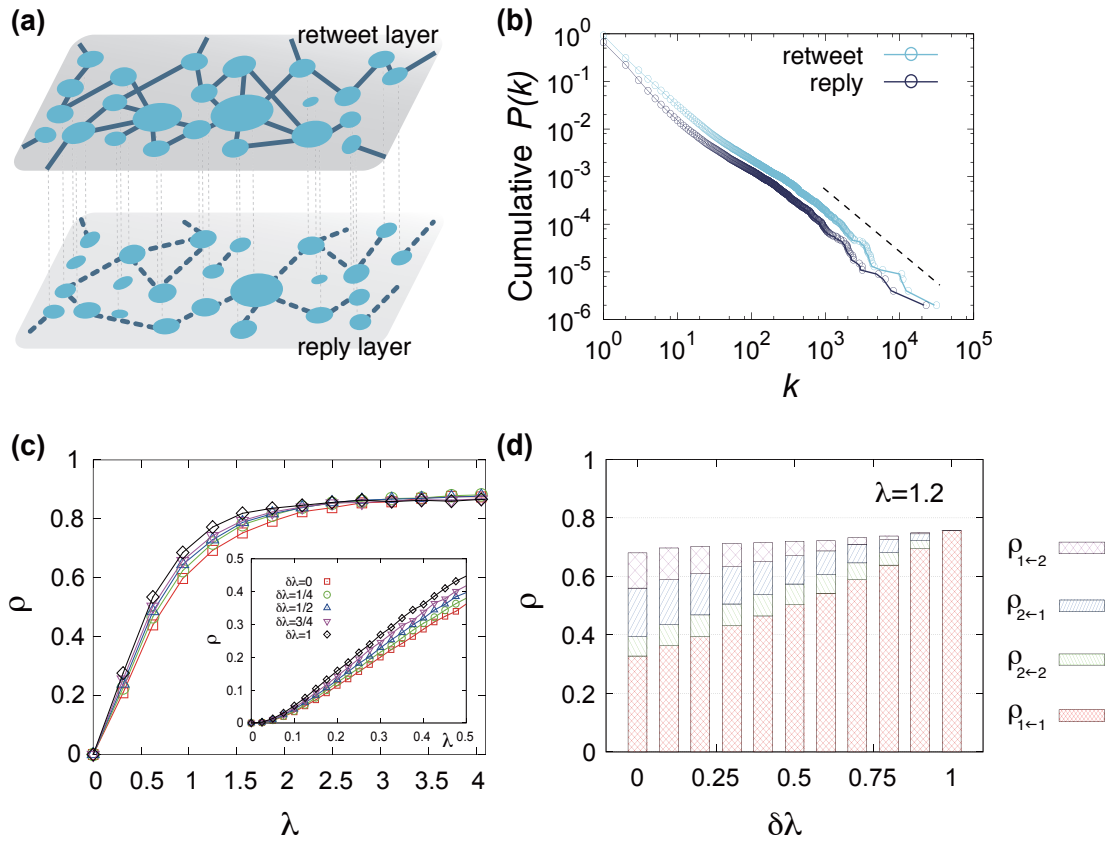


Figure 6. (a) Sample snapshot of a small portion of the 2-layer Twitter network. One can notice that the retweet layer is denser than the reply layer and a significant portion of links are overlapping across the two layers. Size of the node denotes the degree of the node in that layer. The entire Twitter network data consists of $N = 456,631$ nodes, with the mean degree of each layer being $z_{\text{retweet}} = 3.20$ and $z_{\text{reply}} = 1.92$, respectively. (b) The cumulative degree distribution of the two layers in Twitter network. Data for both layers are fitted to a power law with an approximate exponent ≈ -2.3 (as indicated by the dashed guideline with the slope -1.3). (c) Plots of the prevalence ρ on the Twitter network for various values of $\delta\lambda$. (c, inset) A close-up of the prevalence plot for the range of small λ ($0 \leq \lambda \leq 0.5$). (d) The infection channel profile for the Twitter network with $\lambda = 1.2$ and various values of $\delta\lambda$.

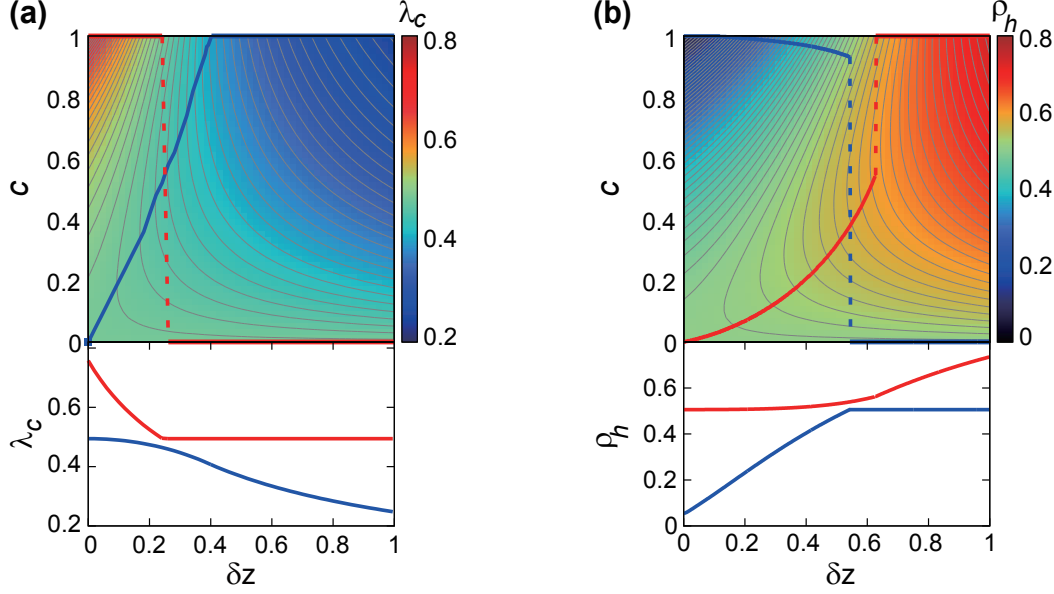


Figure 7. The epidemic threshold λ_c (a) and the prevalence ρ_h for $\lambda = 1.2$ (b) as a function of δz and $\delta \lambda$ for the source layer-dependent spreading model with infection rates Eq. (13) on the duplex ER network with $z_0 = 2.5$ (top panels), and the maximal and minimal values of corresponding observables with respect to $\delta \lambda$ as a function of the given δz (bottom panels). The red (blue) line in top panels represents the loci of maximum (minimum) of the corresponding observables at the given δz , same as in Fig. 3.

epidemic threshold tends lower (Fig. 7, to be compared with Fig. 3). The generalized application of our model framework put forward in this section also suggests a broader formulation of the optimization problem for information spreading in multiplex networks, beyond what has been discussed in comparison with numerical simulations part. For example, the results obtained in this section show that the parameter setting for the source layer-dependent model, Eq. (13), can be more effective in maximizing the information spreading than that with the layer-switching cost, Eq. (12).

Summary and Outlook

In this paper, we have studied an information spreading model framework on multiplex networks with path-dependent transmissibility, paying particular attention to the effect of layer-switching cost. We have formulated a generalized theory to deal with the path-dependent transmissibility and illustrated how the epidemic threshold and prevalence could depend on the layer-switching cost, as well as on the network multiplexity factors such as the link densities of layers and the seed infection channel. Optimal parameters for maximizing prevalence or minimizing epidemic threshold exhibit non-analytic behaviors, reminiscent of the abrupt structural transition in interconnected networks.^{51,52} Our formalism and results show that the seemingly benign factor of layer-switching cost is able to alter the macroscopic dynamic outcome in such nontrivial ways that the multiplex interactions cannot simply be reduced into a single aggregated layer.^{23,30,51} According to our preliminary analysis, the effect of layer-switching cost is observed to be qualitatively similar for another classical epidemiological model, the SIS model,³⁶ as well. Therefore, the network multiplexity should explicitly be taken into account in order to understand and predict spreading dynamics accurately on multiplex networks. To a broader perspective, our results elucidate the impact of path-dependency in spreading process, which can arise also from the presence of memory in temporal networks, the effect of which has recently been studied.^{53–55} Finally, the multiplex information spreading model framework proposed in this paper furnishes us with a versatile platform for more realistic modeling of spreading processes involving layer-wise path-dependent transmissibility on multiplex systems, offering a fertile ground for future study.

Acknowledgments

This work was supported by the National Research Foundation of Korea (NRF) grants funded by the Korea government (MSIP) (No. 2011-0014191 and No. 2015R1A2A1A15052501). K.-I.G. would also like to thank the APCTP for its hospitality during the completion of this work.

Author Contributions

B.M. and K.-I.G. conceived the study. B.M., S.-H.G. and N.L. executed the research. B.M. and S.-H.G. performed the detailed analysis. B.M., S.-H.G. and K.-I.G. wrote the manuscript.

Competing financial interests

The authors declare no competing financial interests.

References

1. M. Chiang, *Networked Life: 20 Questions and Answers* (Cambridge University Press, Cambridge, 2012).
2. F. Salem and R. Mourtada, Civil Movements: The Impact of Facebook and Twitter, *Arab Social Media Report* **1**(2), 1 (2011).
3. J. Borge-Holthoefer, et. al., Structural and dynamical patterns on online social networks: the Spanish May 15th movement as a case study, *PLoS ONE* **6**(8):e23883 (2011).
4. M. De Domenico, A. Lima, P. Mougel, and M. Musolesi, The anatomy of a scientific rumor, *Sci. Rep.* **3**, 2980 (2013).
5. L. M. Verbrugge, Multiplexity in adult friendships, *Social Forces* **57**, 1286 (1979).
6. J. F. Padgett and C. K. Ansell, Robust action and the rise of the medici, 1400-1434, *Am. J. Sociol.* **98**, 1259 (1993).
7. M. Szell, R. Lambiotte, and S. Thurner, Multirelational Organization of Large-Scale Social Networks in an Online World, *Proc. Natl. Acad. Sci. U.S.A.* **107**, 13636 (2010).
8. M. E. J. Newman, *Networks* (Oxford University Press, Oxford, 2010).
9. R. Cohen and S. Havlin, *Complex networks* (Cambridge University Press, Cambridge, 2010).
10. A. Barrat, M. Barthelemy, and A. Vespignani, *Dynamical processes on complex networks* (Cambridge University Press, Cambridge, 2008).
11. G. D'Agostino and A. Scala (eds.), *Networks of Networks: The Last Frontier of Complexity* (Springer, Heidelberg, 2014).
12. M. Kivelä, A. Arenas, M. Barthelemy, J. P. Gleeson, Y. Moreno, and M. A. Porter, Multilayer Networks, *J. Compl. Netw.* **2**, 203 (2014).
13. S. Boccaletti, G. Bianconi, R. Criado, C.I. del Genio, J. Gómez-Gardeñes, M. Romance, I. Sendiña-Nadal, Z. Wang, and M. Zanin, The structure and dynamics of multilayer networks, *Phys. Rep.* **544**, 1 (2014).
14. K.-M. Lee, B. Min, and K.-I. Goh, Towards real-world complexity: an introduction to multiplex networks, *Eur. Phys. J. B* **88**, 48 (2015).
15. R. Pastor-Satorras, C. Castellano, P. Van Mieghem, and A. Vespignani, Epidemic processes in complex networks, *Rev. Mod. Phys.* **87**, 925 (2015).
16. S. Funk and V. A. A. Jansen, Interacting epidemics on overlay networks, *Phys. Rev. E* **81**, 036118 (2010).
17. A. Allard, P.-A. Noël, L. J. Dubé, and B. Pourbohloul, Heterogeneous bond percolation on multitype networks with an application to epidemic dynamics, *Phys. Rev. E* **79**, 036113 (2009).
18. M. Dickison, S. Havlin, and H. E. Stanley, Epidemics on interconnected networks, *Phys. Rev. E* **85**, 066109 (2012).
19. A. Saumell-Mendiola, M. A. Serrano, and M. Boguná, Epidemic spreading on interconnected networks, *Phys. Rev. E* **86**, 026106 (2012).
20. S.-W. Son, G. Bizhani, C. Christensen, P. Grassberger, and M. Paczuski, Percolation theory on interdependent networks based on epidemic spreading, *EPL* **97**, 16006 (2012).
21. J. Sanz, C.-Y. Xia, S. Meloni, and Y. Moreno, Dynamics of Interacting Diseases, *Phys. Rev. X* **4**, 041005 (2014).
22. C. Granell, S. Gómez, and A. Arenas, Dynamical Interplay between Awareness and Epidemic Spreading in Multiplex Networks, *Phys. Rev. Lett.*, **111**, 128701 (2013).
23. E. Cozzo, R. A. Baños, S. Meloni, and Y. Moreno, Contact-based social contagion in multiplex networks, *Phys. Rev. E* **88**, 050801(R) (2013).
24. S. V. Buldyrev, R. Parshani, G. Paul, H. E. Stanley, and S. Havlin, Catastrophic Cascade of Failures in Interdependent Networks, *Nature* **464**, 1025 (2010).

25. J. Gao, S. V. Buldyrev, H. E. Stanley, and S. Havlin, Networks formed from interdependent networks, *Nat. Phys.* **8**, 48 (2012).
26. C. D. Brummitt, K.-M. Lee, and K.-I. Goh, Multiplexity-facilitated Cascades in Networks, *Phys. Rev. E* **85**, 045102(R) (2012).
27. Fei Tan, Yongxiang Xia, Wenping Zhang, and Xinyu Jin, Cascading failures of loads in interconnected networks under intentional attack, *EPL* **102**, 28009 (2013).
28. B. Min and K.-I. Goh, Multiple resource demands and viability of multiplex networks, *Phys. Rev. E* **89**, 040802(R) (2014).
29. S. D. S. Reis, Y. Hu, A. Babino, J. S. Andrade Jr, S. Canals, M. Sigman and H. A. Makse, Avoiding catastrophic failure in correlated networks of networks, *Nat. Phys.* **10**, 762 (2014).
30. K.-M. Lee, C. D. Brummitt, and K.-I. Goh, Threshold cascades with response heterogeneity in multiplex networks, *Phys. Rev. E* **90**, 062816 (2014).
31. J. Yang and S. Counts, Comparing Information Diffusion Structure in Weblogs and Microblogs, in *4th International AAAI Conference on Weblogs and Social Media* (Association for the Advancement of Artificial Intelligence, Palo Alto, 2010).
32. J. Kwon and I. Han, Information Diffusion with Content Crossover in Online Social Media: An Empirical Analysis of the Social Transmission Process in Twitter, in *46th Hawaii International Conference on System Sciences* (IEEE Computer Society, Los Alamitos, 2013) pp. 3292.
33. M. E. J. Newman, Spread of epidemic disease on networks, *Phys. Rev. E* **66**, 016128 (2002).
34. J. C. Miller, Epidemic size and probability in populations with heterogeneous infectivity and susceptibility, *Phys. Rev. E* **76**, 010101(R) (2007).
35. E. Kenah and J. M. Robins, Second look at the spread of epidemics on networks, *Phys. Rev. E* **76**, 036113 (2007).
36. R. M. Anderson and R. M. May, *Infectious diseases of humans* (Oxford University Press, Oxford, 1991).
37. E. A. Leicht and R. M. D'Souza, Percolation on Interacting Networks, arXiv:0907.0894.
38. K.-M. Lee, J. Y. Kim, W.-k. Cho, K.-I. Goh, and I.-M. Kim, Correlated multiplexity and connectivity of multiplex random networks, *New J. Phys.* **14**, 033027 (2012).
39. K.-M. Lee, J. Y. Kim, S. Lee, and K.-I. Goh, Multiplex networks, in *Network of networks* (eds.) A. Scala and G. D'Agostino (Springer, Heidelberg, 2014).
40. B. Min, K.-M. Lee, S. D. Yi, and K.-I. Goh, Network robustness of multiplex networks with interlayer degree correlations, *Phys. Rev. E* **89**, 042811 (2014).
41. L. Feng, C. P. Monterola, and Y. Hu, A simplified self-consistent probabilities framework to characterize percolation phenomena on interdependent networks: an overview, arXiv:1502.01601.
42. S. Melnik, A. Hackett, M. A. Porter, P. J. Mucha, and J. P. Gleeson, The unreasonable effectiveness of tree-based theory for networks with clustering, *Phys. Rev. E* **83**, 036112 (2011).
43. A. Nematzadeh, E. Ferrara, A. Flammini, and Y.-Y. Ahn, Optimal Network Modularity for Information Diffusion, *Phys. Rev. Lett.* **113**, 088701 (2014).
44. S. Nie, X. Wang, and B.-H. Wang, Effect of degree correlation on exact controllability of multiplex networks, *Physica A* **436**, 98 (2015).
45. M. E. J. Newman, Assortative Mixing in Networks, *Phys. Rev. Lett.* **89**, 208701 (2002).
46. R. Pastor-Satorras and A. Vespignani, Epidemic Spreading in Scale-Free Networks, *Phys. Rev. Lett.* **86**, 3200 (2001).
47. B. Min, S. Lee, K.-M. Lee, and K.-I. Goh, Link overlap, viability, and mutual percolation in multiplex networks, *Chaos Soliton Fractal* **72**, 49 (2015).
48. J. P. Gleeson, S. Melnik, and A. Hackett, How clustering affects the bond percolation threshold in complex networks, *Phys. Rev. E* **81**, 066114 (2010).
49. V. Nicosia, G. Bianconi, V. Latora, and M. Barthelemy, Growing Multiplex Networks, *Phys. Rev. Lett.* **111**, 058701 (2013).
50. J. Y. Kim and K.-I. Goh, Coevolution and Correlated Multiplexity in Multiplex Networks, *Phys. Rev. Lett.* **111**, 058702 (2013).
51. S. Gómez, A. Diaz-Guilera, J. Gomez-Gardeñes, C. J. Perez-Vicente, Y. Moreno, A. Arenas, Diffusion Dynamics on Multiplex Networks, *Phys. Rev. Lett.* **110**, 028701 (2013).

52. F. Radicchi and A. Arenas, Abrupt transition in the structural formation of interconnected networks, *Nat. Phys.* **9**, 717 (2013).
53. M. Rosvall, . V. Esquivel, A. Lancichinetti, J. D. West, and R. Lambiotte, Memory in network flows and its effects on spreading dynamics and community detection, *Nat. Comm.* **5**, 4630 (2014).
54. I. Scholtes, N. Wider, R. Pfitzner, A. Garas, C. J. Tessone, and F. Schweitzer, Causality-driven slow-down and speed-up of diffusion in non-Markovian temporal networks, *Nat. Comm.* **5**, 5024 (2014).
55. P. Holme and N. Masuda, The basic reproduction number as a predictor for epidemic outbreaks in temporal networks, *PLoS ONE*, **10**, e0120567 (2015).